Liquid-helium temperature long-path infrared spectroscopy of molecular clusters and supercooled molecules

Sigurd Bauerecker[a] and Michael Taraschewski
Institut für Physikalische und Chemische Analytik, GKSS-Forschungszentrum GmbH, Max-Planck-Strasse, D-21502 Geesthacht and Institut für Physikalische und Theoretische Chemie, Technische Universität Braunschweig, Hans-Sommer-Strasse 10, D-38106 Braunschweig, Germany

Claus Weitkamp
Institut für Physikalische und Chemische Analytik, GKSS-Forschungszentrum GmbH, Max-Planck-Strasse, D-21502 Geesthacht, Germany

Heiko K. Cammenga
Institut für Physikalische und Theoretische Chemie, Technische Universität Braunschweig, Hans-Sommer-Strasse 10, D-38106 Braunschweig, Germany

(Received 15 May 2001; accepted for publication 18 June 2001)

Collisional cooling and supersonic jet expansion both allow us to perform infrared spectroscopy of supercooled molecules and atomic and molecular clusters. Collisional cooling has the advantage of higher sensitivity per molecule and enables working in thermal equilibrium. A new powerful method of collisional cooling is presented in this article. It is based on a cooling cell with integrated temperature-invariant White optics and pulsed or continuous sample-gas inlet. The system can be cooled with liquid nitrogen or liquid helium and operated at gas pressures between $<10^{-5}$ and 13 bar. Temperatures range from 4.2 to 400 K and can be adjusted to an accuracy of ± 0.2 K over most of the useable range. A three-zone heating design allows homogeneous or inhomogeneous temperature distributions. Optical path lengths can be selected up to values of 20 m for Fourier transform infrared (FTIR) and 40 m for laser operation. The cell axis is vertical, so optical windows are at room temperature. Diffusive trapping shields and low-power electric heating keep the mirrors free from perturbing deposits. The cell can be operated in a dynamic buffer-gas flow-cooling mode. A comprehensive review of existing collisional cooling cells is given. The formation of CO clusters from the gas phase was investigated using FTIR spectroscopy. For the isotope mixture consisting of $^{13}C^{16}O$,$^{13}C^{18}O$, and $^{12}C^{16}O$, a conspicuous change in the main spectroscopic structure of the clusters was observed between 20 and 5 K. The cluster bandwidth of the main isotope $^{13}C^{16}O$ triples. This behavior could be interpreted as a change from the crystalline to the amorphous state or as a decrease in size to smaller clusters with relatively larger surfaces. To our knowledge, this is the first IR investigation of molecular clusters obtained by collisional cooling in this temperature range. For CO_2 the change from the monomer to crystalline clusters was investigated. The observed spectra vary considerably with temperature. FTIR spectra of CO_2 clusters observed previously by other researchers could be reproduced. The system allows us to determine various gases with a FTIR detection limit in the lower ppb range. With these concentrations and at temperatures <10 K the monomers can be supercooled, and small clusters can be obtained. [DOI: 10.1063/1.1400158]

I. INTRODUCTION

Cooling and supercooling of molecular gases offer a number of possibilities not given at room temperature. Lines and bands get narrower and hot bands disappear due to the strong temperature dependence of Doppler and collision linewidths and of the Boltzmann population of J states. So the spectra become simpler and individual lines get stronger. Low-temperature high-resolution spectroscopy[1] including tunable diode laser (TDL) spectroscopy[2] can thus be used for the analysis of gas mixtures with complex spectra, particularly for heavy molecules with small rotational constants and narrow-spaced lines. Laboratory measurements can provide basic information on spectral properties such as linewidth, line strength, and absorption cross section. These data may be used for the optical investigation of the Earth's atmosphere as well as the atmospheres of other planets.[3] Interesting fields of research are also the investigation of chemical reactions with a large negative temperature coefficient of the rate constant[4] and the violation of parity conservation in chiral molecules.[5]

If the temperature of a gas is reduced below its condensation point and its supersaturation is raised above a value of five,[6] then aggregation can occur. Most cooling methods are therefore suited for the generation of molecular clusters as

[a]Author to whom correspondence should be addressed; electronic mail: sigurd.bauerecker@gkss.de

well.[7–12] The study of homogeneous and heterogeneous molecular clusters provides basic knowledge about solids and liquids, although clusters themselves are sometimes considered as a new state of matter because of the great variety of physical and chemical properties they exhibit. Due to their large specific surface, clusters can act as efficient catalysts in atmospheric chemistry as well as in chemical and biochemical applications. In addition to these cluster-specific reactions, research into the behavior of clusters could contribute to answer questions of fundamental and practical importance in fields such as nucleation phenomena, phase transitions, and solvation problems. In cluster research, theory and simulation are far ahead of the experiment. Berry[13] therefore calls for increased effort and new laboratory studies in this field, particularly as to phase changes of small systems.

Experimental cooling methods suited for the purpose include supersonic adiabatic expansion into vacuum, collisional cooling, and matrix isolation.[14,15] This latter method differs from the two former ones in that the solid matrix of (usually) argon strongly interacts with both the monomers and the clusters, rendering statements about the bare molecules and clusters difficult. Considered to be the more elegant, adiabatic jet expansion[1,16] is used much more frequently than collision cooling. Adiabatic expansion does not depend on a cooling agent and allows us to attain monomer rotational temperatures of a few K under controlled experimental conditions. The problem of low intensity can to a certain extent be overcome by the use of slit instead of circular nozzles, particularly if spectrum acquisition is synchronized with the pulses of the molecule jet.[17,18] On the other hand, supersonic expansion requires large amounts of sample gas which in turn calls for large-capacity vacuum pumps. Also the definition of temperatures of the carrier gas, the sample gas, and the aggregates is not obvious because the system is far from thermal equilibrium and the vibrational relaxation lags behind the rotational and translational relaxation processes.[19] Therefore, researchers have repeatedly come back to collision cooling devices, all of which essentially consist of a suitably designed cooling cell.

II. EXISTING COLLISIONAL COOLING CELLS

Herzberg[20] was the first to use a cooled optical cell for spectroscopic purposes in 1952. It was cooled with liquid nitrogen (LN_2). Thirteen years later a high-performance cell with a minimum temperature of 18 K was described,[21] which offered an optical path length of 13.6 m. It was based on White's design[22] as were all the following multireflection cells. Watanabe's cell operated at pressures slightly above 1 bar. A coarse adjustment of the temperature was possible by letting the cell slowly warm up to room temperature. The cell was used for the determination of pressure-induced infrared (IR) absorption by gaseous H_2. A few years later two long-path cooling cells were built with optical lengths of 230 and 165 m, minimum temperatures of 77 and 80 K, and maximum pressures of 3 and 10 bar, respectively.[23,24] The temperature of the latter of the two cells could be adjusted between 80 and 125 K by use of a cryogenerator that worked with a liquid coolant such as nitrogen. Based on this design, another cell was built with 110 m of optical length that could be cooled down to 20 K with a two-stage cryogenerator.[25,26] However, this cell could not be used for IR absorption measurements for more than 1 or 2 days because of a deposit of water vapor on the outside of the cold vacuum windows.[26] The previously mentioned 230 m cell[23] was used both in the original[27] and in a smaller version[28] to spectroscopically investigate large CO_2 clusters in the IR at 77 K. For this purpose, mixtures of CO_2 with an inert gas were allowed to quickly enter the cold cell. Two other cells offering very long absorption paths of 1500 and 512 m were described for temperatures between 160 and 300 and 190 and 300 K, respectively;[29–31] maximum pressure in these cells was 5 bar. For high resolution spectroscopy of the HF dimer a double-jacketed, stainless-steel 64 m path White cell, which was cooled down to about 223 K, was used.[32] A 10 m double-path cell was also built for experiments with highly aggressive media and used for the investigation of gaseous HF and its smaller clusters at temperatures between 250 and 300 K.[33]

After 1989, a number of smaller cooling cells were described that could be integrated into the sample compartment of commercial Fourier transform infrared (FTIR) spectrometers. They were all single-pass cells with a length of $<0.02–0.25$ m. The first of these cells used the diffusive trapping technique.[34] The LN_2-cooled cell was given the shape of a long (≈ 0.1 m) cylinder so that supercooled sample gas entering the cell in the center condensed mainly on the cylinder walls and to a much lesser extent on the two windows. This technique allowed measurements for about 6 h before the deposit on the windows set an end to the experiment; temperatures that could be reached were about 90 K. The cell was used for the investigation of both the behavior of supercooled gases[33] and the formation of homogeneous[35–37] and heterogeneous[38] clusters. Simultaneously or soon thereafter three similar cells were built and described. The first,[39] with 0.09 m optical length, was used for high-resolution IR spectroscopy of CH_3D at 123 K. With the second, 0.15 m long, based on diffusive trapping and resembling the cell described in Refs. 23 and 27, FTIR spectroscopy of CO_2 aggregates[40] and of homogeneous[41] and heterogeneous H_2O aggregates[42] were carried out; this cell could go down to temperatures <90 K. Finally, a third cell of 0.1 m optical path and 95 K minimum temperature and a longer version of it (0.2 m and 30 K) were used for FTIR studies of C_2H_2 (Ref. 43) and N_2H_4 (Ref. 44) clusters. In 1995 a similar cell made from Pyrex glass was described that was 0.25 m long, resistant to aggressive media, could be cooled to 77 K and heated electrically, and was used for FTIR spectroscopy of gaseous CO_2,NO_2,CH_3SiH_3,[45] and several fluorohydrocarbons.[46]

Somewhat longer cells of 0.32 and 0.50 m have been used for N_2O at 135 K and CH_4 at 210 K, respectively.[47,48] Pressure broadening of CH_4 was investigated at temperatures down to 77 K with a 0.85 m long tubular cell, the central part of which was surrounded by a Dewar that could be filled with liquid nitrogen.[49] A different design was used for a cell for IR spectroscopy of various aerosols. This cell consisted of a copper tube, 0.8 m long and 0.1 m in diameter, with four different zones each of which could be cooled to a different

temperature, and three ports in-between through which the aerosol could be investigated optically in a direction perpendicular to the cell axis. In this cell water ice aerosol was studied along optical paths of about 0.2 m in the temperature range between 130 and 210 K.

The only cell that has, to our knowledge, been described in the literature for IR spectroscopy of supercooled monomers and molecular clusters at liquid helium temperatures is the device of Refs. 50–52. It combines helium cooling with microwave measurement capabilities and was used for the determination of pressure broadening coefficients[53–56] and rotationally inelastic absorption cross sections[57] of several gas systems. A precursor of this cell had been directly coupled to a microwave detector, with both the cell and the detector immersed in liquid helium.[58] The cell was quite small, with an effective optical path of about 25 mm, but could be cooled to 7.5 and 5 K for TDL spectroscopy of individual lines of CH_3F (Ref. 50) and N_2O.[51] A slightly modified version that offered 42 mm of optical path at a temperature of 14 K has been used for IR measurements on CO.[52]

All these devices can be improved as to both methodology and technology. An important capability arises from the combination of liquid helium temperatures with an optical path of several meters. At the same time, operation of the cell must not be too complicated and time consuming. Furthermore, the possibility to precisely and continuously control the temperature between a few K and a few hundred K is highly desirable. A low-loss sample-gas inlet system is essential for many practical applications. Except for one cell[21] all cooling cells described in the literature were oriented in the traditional way, with the cell axis horizontal. This leads to cold gas flowing to the windows and cooling them and results in a temperature gradient in the windows. The cold windows tend to accumulate condensed sample gas inside and condensed water vapor outside. This limits the time of the experiment, requires periodic heating, and renders the interpretation of the results difficult. It can also provoke leaks around the windows, particularly while the cell is cooled down. Furthermore, certain window materials are hygroscopic (such as KBr) or susceptible to thermal shock (such as BaF_2). Finally, especially for multipath cells, provision for heating the mirrors is important to avoid the deposit of gas on the mirrors or to remove it without heating up the whole system. None of the systems that we found described in the literature provides this possibility. A fundamental problem is also the temperature-induced change of length of cells made from copper, brass, or steel; this phenomenon complicates the optical readjustment of the mirrors when the cell is cold.[23] A solution is the use of invar steel which has an expansion coefficient similar to that of glass, but ten times its thermal conductivity.

III. COOLING TECHNIQUE

A concept to avoid the deposit of sample gas on windows, mirrors, and walls of the cooling cell has been described by the authors previously.[59,60] This concept relies on cooling and channeling the sample gas with a flow of cold, noncondensing buffer gas. Its viability has been proven with a double-path cell cooled with liquid nitrogen.[61–63] In this article a new, versatile cell is described which allows us to realize the aims described above, eliminates the remaining shortcomings of the older cell, and opens possibilities beyond those offered previously.

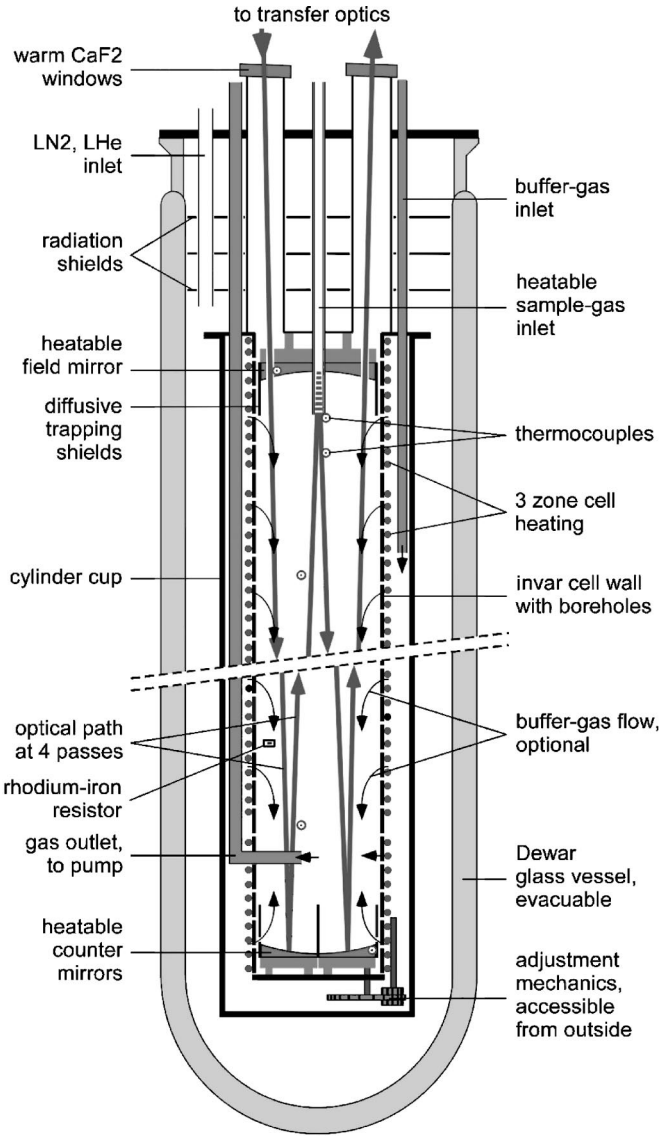

FIG. 1. Schematic cross section of the liquid-helium/liquid-nitrogen cooled multireflection cell. The efficiency of the method used lies in the combination of (1) liquid helium cooling, (2) up to 20 m (FTIR) or up to 40 m (TDL) optical path length, (3) three-zone temperature heating with independent temperature control of each zone, (4) absence of sample gas deposits on windows and mirrors, and (5) a new sample-gas inlet system for continuous or pulsed operation.

The central part of the new device is a vertically oriented multireflection cooling cell with long necks to carry the optical windows (Fig. 1). The cell is combined with a new gas inlet system that can be operated both continuously and in a pulsed regime. The inner volume of the cell is contained in an invar steel tube with integrated $f/16$ White optics.[22] The distance between the gold-coated mirrors is 0.625 m so the optical path can be changed in multiples of 2.5 m. The adjustment is carried out by tilting one of the mirrors at the base of the cell with a rod that can be actuated from outside the cell. Adjustment of the cell optics is thus possible at any

cell temperature. In practice, however, no realignment was necessary when the cell was cooled from room temperature to the minimum operating temperature of the device. Maximum optical pathlength is 20 m for FTIR and 40 m for TDL operation. A stainless steel cap at the top seals the inner cell against the top flange with an indium gasket. This is the only gasket of the whole device that must endure temperature changes while the cell is cooled. All other gaskets for windows, inlet, and exhaust tubes, etc. are kept at room temperature, so no leak problems occur. The cryostat that surrounds the cell is made of Duran glass with thermal conductivity only 1/10 that of stainless steel. The cryostat can thus not only be operated with liquid nitrogen, but with liquid helium as well if an appropriate radiation shield is added.

Compared to a horizontal arrangement, the vertical orientation of the cell offers some advantages. Most important is that the temperature gradient from the outside to the inside of the cell occurs in the window necks which only contain a buffer gas such as nitrogen or helium which do not condense. Because of the higher density of the colder gas there is a stable layering in the necks that keeps cold gas from flowing to the windows, unlike the situation in cells with a horizontal axis. The windows thus remain at room temperature. No deposit occurs on the windows either from the inside or from the outside. As a window material, both CaF_2 and KBr are used. The windows are secured in the flanges with bolts. Flanges are tilted 3° with respect to the optical axis.

The sample gas enters the cell along the cell axis from the top. For its introduction several interchangeable tubes are available. The tubes are introduced into a larger tube that provides mechanical stability and pass through a central hole in the field mirror over which they stand out into the cell by up to 60 mm (Fig. 1). Thus, they do not impair the optical beams focused on the field mirror. We use thin-walled, vacuum-isolated glass or stainless-steel tubes with outside diameters of 10 mm and inner diameters between 2 and 4 mm. The glass tubes introduce less heat into the cell than do the steel tubes.

Two possibilities exist for the injection of the sample gas: continuous injection and pulsed injection. For continuous operation the sample gas flow is adjusted via mass-flow controllers. Another possibility is the quick introduction of short gas pulses of variable length into the cooling cell. For this purpose a sample gas pressure between 0.1 and 10 bars is allowed to build up in an adjustable, well-defined volume of a few to a few hundred cubic centimeters. An electric pulse generator with adjustable pulse length and pulse repetition frequency then opens a valve. Minimum pulse duration and maximum pulse repetition frequency are determined by the switching time of the valve which is 60 ms. At high pressure and short pulse duration the sample gas enters the cell at high speed, and very little gas can condense in the inlet tube. The sample gas concentration, the pressure in the gas reservoir, the pulse length, the diameter and nozzle shape of the inlet tube, the degree of turbulence at which the sample gas enters the cell, and the temperature of the buffer gas all have considerable influence on—and are thus allowed to influence—the size and probably the shape of the resulting clusters.[64] With the pulse generator the phase-controlled injection of up to five separate gas pulses can be used for the generation of multicomponent molecular clusters.[64]

The buffer gas enters the space between the steel cap and the invar tube through the buffer-gas inlet pipe (Fig. 1). Here it is cooled, and possible impurities condense on the metal surfaces. After that the gas smoothly flows into the inner cell through 2000 holes laser drilled into the invar cylinder. The cell can be operated in two different modes. In the static mode the sample gas is injected into the cell prefilled with buffer gas. In the dynamic mode the buffer gas forms a laminar, rotationally symmetric flow pattern that is schematically represented in Fig. 1. In the upper part the buffer gas enters the cell essentially radially, then gradually turns into a more axial direction, and finally flows parallel to the cell axis toward the gas outlet tube. In that option the cooling gas surrounds and carries the sample gas through the cell, cooling it and keeping it off the cylinder walls, where it might otherwise condense and deposit. Part of the cooling gas flow flushes the mirrors at the top and bottom of the cell, avoiding or drastically reducing the deposit of sample gas on the mirrors. This is particularly important when sample gas concentrations in excess of 10–100 ppm are used. An additional possibility is the addition of a third gas to the buffer gas. This can be used for the study of heterogeneous clusters and multicomponent reactions as an alternative to the multipulse injection of different gases.

IV. TEMPERATURE ADJUSTMENT

Two systems are available for cell temperature control. Temperatures between 100 and 400 K are obtained using a device that allows us to adjust the temperature of gaseous nitrogen evaporated from the liquid in a heat exchanger. The temperature of the gas obtained by this procedure can be controlled to an accuracy of better than ± 0.2 K. Maximum cell temperature is given by the melting temperature of the indium gasket (430 K).

For temperatures between 4.2 and 200 K liquid helium (4.2–78 K) and liquid nitrogen (78–200 K) are used, together with electric heating of the mirrors and of the invar tube. For this purpose insulated heating wire is wound around the invar tube (Fig. 1). The heating is arranged in three segments. Each can deliver, at 48 V, a maximum heating power of 200 W. Care has been taken that the heating wire does not impair the free passage of the buffer gas through the holes. Close to the evaporation temperature of nitrogen, i.e., in the range between 78 and 85 K, stability and precision of the temperature is ± 0.1 K. When helium is used, radiation shields are required in the upper part of the cell close to the window necks to avoid radiation heating of the inner parts of the device.

Temperatures above about 60 K are measured in seven positions (one at the sample-gas inlet, four in the gas in the cell, two at the mirrors) and controlled by self-optimizing fuzzy-logic controllers. In the inner hole of each sample gas inlet tube there are two chromel–alumel mantle thermocouples with stainless-steel mantle. With one of the thermocouples the gas temperature is measured at the tip of the inlet tube. The other serves for heating the sample gas. Its power

is carefully adjusted to the cell temperature and to the nature, flow, and concentration of the sample gas to avoid clogging of the sample gas inlet.

Gas temperatures in the cell are measured directly with a rhodium–iron resistor and three chromel–alumel mantle thermocouples with a stainless-steel mantle. The outside diameter of the thermocouples is 0.5 or 0.25 mm. According to the manufacturer, these thin thermocouples have response times (63% response to an abrupt temperature change) of 1.2 or 0.4 s, respectively, measured in nitrogen at atmospheric pressure. The thermocouples radially protrude about 40 mm from the invar tube into the cell volume. They are located at the top, middle, and bottom of the cell. The resistor is located at a position between the middle and the lower thermocouple. The remaining two thermocouples measure the surface temperature of the field mirror and one of the focusing mirrors.

Temperatures between 4.2 and 60 K are measured with the rhodium–iron resistor and additionally verified with a pressure measurement by use of the van der Waals' relation with calibration of the system at 77.4 and 4.2 K.

The field mirror at the top and the pair of focusing mirrors (counter mirrors) at the bottom of the cell can each be heated electrically with 100 W of heating power. This allows, e.g., us to heat the mirrors from 78 to 300 K in 20 min while the cell is immersed in liquid nitrogen. A deposit of gas on the mirrors can be totally avoided if the temperature of the mirrors is a few K higher. This has practically no influence on the temperatures of the sample gas as given by the three thermocouples in the cell. It is also possible to have the mirrors at temperatures below the sample-gas temperature. In this way thin layers of deposit can be made to grow on the mirrors and to evaporate again in a controlled manner for the study of processes associated with changes in structural order. In addition to the mirror heating, diffusive trapping shields—following the diffusive trapping technique—[34] are also used to avoid sample gas condensation on the mirrors. These are fan-shaped adsorption baffles that consist of four aluminum sheets for the top mirror and two tubular baffles for the bottom mirrors. For improved adsorption of gas molecules the surface of the aluminum is roughened.

Maximum pressure of the cell is determined by the mechanical properties of the cell windows. Following the calculations carried out in Ref. 31, the maximum pressure of our cell is at least 13 bars when operated with 5-mm-thick CaF_2 windows at a safety factor of 2. Minimum pressure is below 0.01 mbar.

V. EXPERIMENTAL RESULTS

The experimental setup is shown in Fig. 2. A Nicolet Magna-550 FTIR spectrometer was used to obtain the results presented in this article, with a globar mid-infrared source. Maximum resolution in the spectral range between 600 and 7400 cm^{-1} is 0.125 cm^{-1}. A KBr beamsplitter produces a sample beam that comes out of the spectrometer parallel to the reference beam. A transfer optics couples the beam down into the cooling cell. The attenuated beam that comes out of the cell is measured with a mercury–cadmium–telluride or indium–antimonide (InSb) detector. To enhance optical throughput in the spectral region of interest, yet reduce unwanted photon noise, an optical filter transmitting in the 2000–2500 cm^{-1} range was used in most cases. For all IR spectra shown in this article Happ–Genzel apodization was used along with zero-filling-level-of-two algorithm. Raw interferograms were always stored for reevaluation at a later date. In order to suppress absorption bands of H_2O and CO_2, the spectrometer and transfer optics were flushed with dry nitrogen.

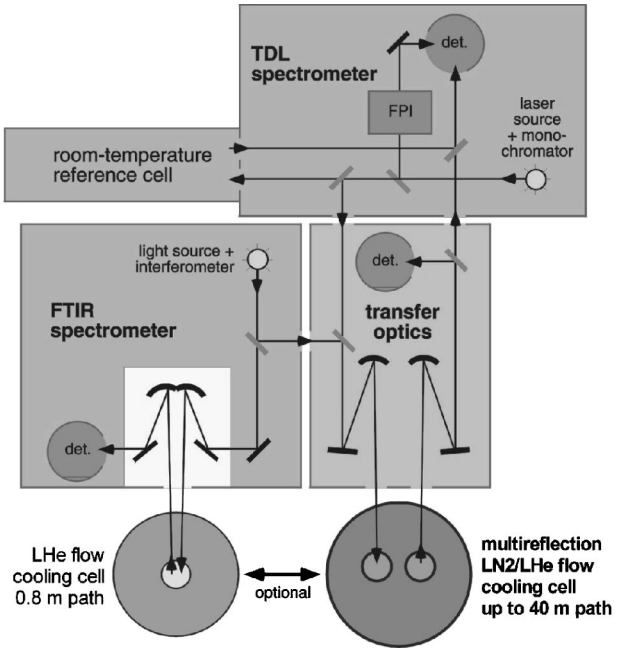

FIG. 2. Experimental arrangement with transfer optics. The system allows operation of the FTIR and TDL spectrometers on either of two cooling cells. The 0.8 m path liquid-helium flow-cooling cell on the lower left is not described in this work.

For high-resolution IR spectroscopy a TDL spectrometer can be coupled to the cooling cell. For this purpose only two mirrors in the transfer optics are removed from the beam. Simultaneously with the multipath absorption cell described here, a helium-cooled double-path cell can be operated when using a second coupling device integrated into the sample compartment of the FTIR spectrometer. That cell is equipped with a very long window neck and a LN_2-cooled mantle cryostat and is thus even less subject to heat input from the surroundings than the multireflection cell. It is not discussed in this work. All gas mixtures used had been prepared by Messer and came in 10 l pressure cylinders with an analysis certificate. Concentration uncertainty was quoted to be $\pm 2\%$. Teflon was exclusively used for all external tubing. Flow rates of the sample and of the cooling gas were measured with mass flow controllers.

A. Carbon monoxide clusters

With 81.7 K, carbon monoxide exhibits the lowest atmospheric-pressure boiling point of all (nonexotic) IR-active molecules.[65] Therefore, CO is well suited as a model substance for the IR spectroscopic investigation of cluster formation at temperatures below 78 K. Although IR spectra of cooled CO monomers[16,52] and heterogeneous CO clusters,

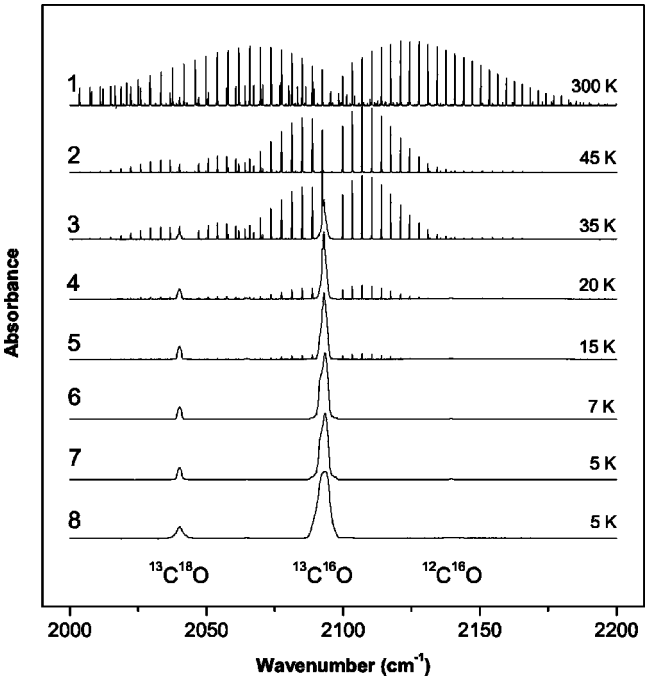

FIG. 3. FTIR spectra of CO clusters. Temperature series between 300 and 5 K. "Cold" spectra were obtained after injection of three (Nos. 2–5) and four (Nos. 6–8) pulses, of 50 ms pulse duration, of a mixture of 1000 ppm CO in helium. CO isotopic composition was $^{13}C^{16}O$,$^{13}C^{18}O$,$^{12}C^{18}O$ at a ratio of 100:10:0.7. The pressure of the cold buffer gas into which the sample gas pulses were injected was 25, 18, 15, 12, 8, 7, and 7 mbar. No buffer gas flow was used. The maximum absorbances were, from No. 1 to 8: 0.37, 0.19, 0.15, 0.42, 0.38, 0.59, 0.27, and 0.11. Optical path length was 20 m, spectral resolution was 0.125 cm^{-1}. Cluster formation started at about 40 K.

e.g., with H_2O,[42,66] have been presented, articles on infrared spectra of homogeneous CO complexes appear to be scarce, except for high-resolution spectra of jet cooled CO dimers.[67] The cooling system described offers the possibility of producing CO clusters with a great variety of properties by varying the concentration, pressure, and temperature and to spectroscopically investigate them in thermal equilibrium. Figure 3 consists of a series of eight CO spectra taken at temperatures that range from 300 down to 5 K. In all eight experiments the concentration was 1000 ppm of a $^{13}C^{16}O$ enriched CO isotope mixture in helium. Isotopes $^{13}C^{16}O$, $^{13}C^{18}O$, and $^{12}C^{18}O$ are present in the sample gas in a proportion of 100:10:0.7. At 300 K the empty cell was filled with a sample gas mixture up to 50 mbar pressure. In the seven remaining experiments three (Nos. 2–5) and four (Nos. 6–8) pulses of gas were introduced into the cell that was at a temperature of 45, 35, 20, 15, 7, 5, and again 5 K. The corresponding pressure values were 25, 18, 15, 12, 8, 7, and once again 7 mbar. Three seconds after the third pulse the absorption measurement was started, always at 20 m optical path, and carried out in eight scans extending over a total of 63 s, with 0.125 cm^{-1} spectral resolution. The difference between the seventh and eighth run was that only 60% of the sample gas volume of run No. 7 was allowed to enter the cell in run No. 8. For this purpose the gas reservoir pressure was reduced accordingly.

As can be seen from the first two spectra of Fig. 3, the temperature reduction from 300 to 45 K results in a reduction of the rotation–vibration bandwidth to about 40% its initial value. This is a considerable spectral simplification. Cluster formation starts between 45 and 35 K. At these temperatures the equilibrium vapor pressure of CO is between 10^{-1} and 10^{-3} mbar, in agreement with the partial pressure of CO in the cell, which after three gas pulses is between about 10^{-2} and 10^{-3} mbar. It is worth mentioning that the temperatures cannot be taken directly from the monomer bands or lines of the spectra as the widths of the lines are about ten times smaller than the spectral resolution of 0.125 cm^{-1}. Monomers totally disappear between 15 and 7 K. Cluster spectral structures of the three isotopes are redshifted by 3–4 cm^{-1} with respect to the bands of the monomer.

For the interpretation of the cluster spectra let us start with spectra Nos. 7 and 8 taken at 5 K. Despite the fact that the melting temperature of clusters can considerably decrease with decreasing size[68] and that the probability for the occurrence of several phases is larger in small systems because of the relatively larger surface and the greater variety of simultaneously occurring cluster sizes, we can be rather confident that these two spectra are from solid clusters only. There are several reasons for this. At 5 K, CO is far below its triple point at 68.1 K and on a point along the sublimation curve of its p–T phase diagram in which the vapor pressure essentially vanishes.[65,69] For CO_2 a concentration of 1000 ppm and similar pulse conditions result in clusters of 10^8–10^9 molecules per cluster, as is described below with consideration of Ref. 28. This can be taken as an indication that CO clusters are not very small under these conditions. On the other hand, the absence of scattering noise and any Christiansen effects is indicative of a cluster size considerably below the IR wavelength of about 5 μm.[43]

Figure 4 shows the structure of the $^{13}C^{16}O$ stretching vibration of spectra Nos. 4–8 of Fig. 3 in more detail. Two shoulders at 2091.8 and 2094.0 cm^{-1} can be seen in the center and three, less clearly developed shoulders at 2088.2, 2089.8, and 2097.2 cm^{-1} in the outer parts of the spectra. All of them get more pronounced as the temperature gets lower. Together they lead to a broadening of the spectral structure both in the central and in the outer regions. Most conspicuous is the spectral broadening by about 50% between Nos. 7 and 8. Most of the structural change thus occurs between these two spectra. This is amazing because both temperature and pressure have remained the same for the two spectra. It means that only the reduced quantity of sample gas can be held responsible for the change in structure. We feel confident that the effect described is not an artifact. At homogeneous mixing of the sample gas during the measurements and maximum absorbances of 0.27 and 0.11, saturation effects can safely be excluded. Also the experiment was repeated several times with the same results.

The 40% reduction of the pulsed-in gas quantity appears to cause two things. First, the sample gas becomes more strongly diluted. Fewer sample gas molecules meet the same number of cold buffer gas atoms. Second, the sample gas is cooled more quickly as a smaller gas mass must be cooled. Because the average time between collisions is inversely proportional to the molecular number density and the square root of the temperature, both effects cause longer and thus

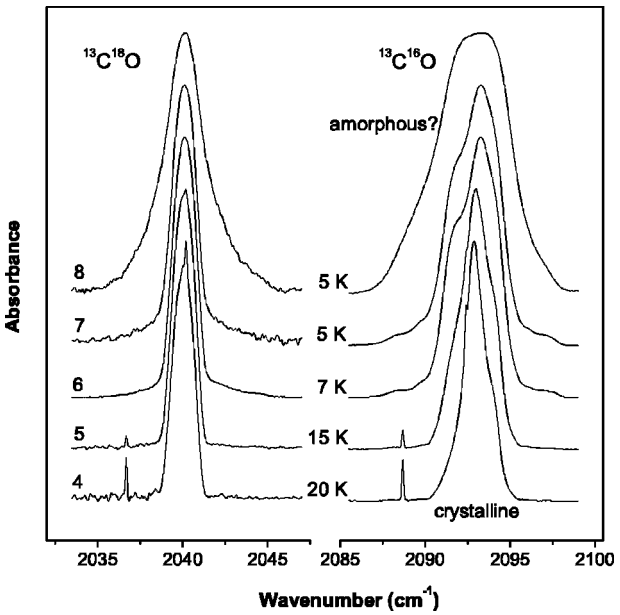

FIG. 4. Details of the FTIR spectra of CO clusters from Fig. 3. Temperature series between 20 and 5 K, in opposite order. Decreasing temperature causes the maximum of the $^{13}C^{16}O$ cluster peak to shift toward the blue by about 0.5 cm^{-1}. The $^{13}C^{16}O$ spectral features triple and the $^{13}C^{18}O$ features double in width with the decrease in temperature. The change occurs essentially between spectra Nos. 7 and 8 at about 5 K, in particular for $^{13}C^{18}O$; for spectrum No. 8 the pulse volume had been reduced to 60%. This behavior could be interpreted as a change in structural order of the clusters and/or as an increase of the surface-to-volume ratio of the clusters. The different development of the spectral features of the two isotopes can be explained by different phonon coupling.

stronger cooling of the monomers before they collide and aggregate with each other or with a cluster already formed there. That means that the clustering process occurs at lower temperatures in run No. 8 than in run No. 7. This results in an increased probability for the formation of a glassy structure.[68]

It was observed[70] that the amorphous as compared to the crystalline part of H_2O clusters is relatively larger in smaller clusters. Because rapid cooling results in a higher level of supersaturation, which in turn leads to higher rates of nucleation and thus to smaller clusters,[71] a similar situation could be given in the present case. The peaks of the cluster spectra of isotope $^{13}C^{18}O$ (Fig. 4, left) are only about half as broad as those of the main isotope. It is noteworthy that the shape of the spectra of this isotope remains almost the same between run Nos. 4 and 7, differently from the behavior of the main isotope. Considerable broadening only occurs in the transition from No. 7 to No. 8. The spectra of $^{12}C^{18}O$ (not shown here in greater detail) correspond very well to the spectra of $^{13}C^{18}O$ and thus behave in a very similar way. This is explained by the fact that the minority isotope is surrounded mainly by molecules of the main isotope and that coupling of vibrational excitation is much more intense between like than between unlike molecules. The smaller changes in the spectral structure of the minority species have also been observed with CO_2 clusters and explained using the exciton model.[28] In that experiment clusters were also produced by collisional cooling at 77 K and turned out to be all crystalline. The transition to a broader structure, however, as seen in this investigation, had not been observed there. In summary, we thus interpret the transition in spectra structure between run Nos. 4 and 8 as a change from crystalline toward an amorphous phase of the forming clusters and/or as a decrease in size to smaller clusters with relatively larger surface areas.

B. Carbon dioxide clusters

Whereas very little information has so far been available on clusters of CO, IR spectra of larger CO_2 clusters have been presented in several articles.[27,28,35–37,40] These articles are therefore suited for the verification of the quality of data obtained by using our new technique, although the influence of temperature on cluster formation has not been a prime topic there.

Figure 5 shows, in three columns, CO_2 spectra taken with sample gas concentrations of 1002, 91, and 11 ppm CO_2 in helium. An exception is the bottom spectrum in the right-hand column which was taken with 10 600 ppm of CO_2. The temperature was lowered in small steps from top to bottom, starting from a value between 100 and 90 K and going down to 78 K. The sample gas was always pulse injected into the cooling cell which was filled with 200 mbar of helium buffer gas and homogeneously kept at the adjusted temperature. The first series of spectra was taken with one, the second with two, and the third with five pulses under otherwise identical conditions. Again spectra acquisition started 3 s after the end of the last injection pulse, optical path length was 20 m, spectra were taken in 15 scans each, with a total duration of 118 s, and resolution was 0.125 cm^{-1}. It is obvious that cluster formation onset occurs at about 95 K in the first series, at about 91 K in the second, and at roughly 89 K in the third series of measurements. Further cooling by only a few degrees strongly enhances the cluster part in the spectra, yet monomers and clusters coexist. Around 85, 84, and 80 K the monomers disappear almost completely. (Spectra *F* and *G* of the first series have been arranged according to structural trend, not temperature. They seem to deviate from the leading trend, but no data interchange nor any other error could be found in the acquisition and evaluation of the primary experimental data.)

For all three concentrations the structure of the cluster bands formed strongly depends on temperature. It is interesting to note that the IR spectra of the three sequences of measurements very closely resemble the results of four experiment series obtained by three working groups that used different cooling systems. Our spectrum *D* matches quite well with that obtained in Ref. 35 for a cluster size distribution, which according to the authors has a maximum near 10^9 molecules per cluster; clusters of this size should have a particle radius of about 0.25 μm. Our spectrum *H* resembles several spectra discussed in Ref. 28 with clusters of around 0.1 μm size in the maximum of the distribution. Spectra *F* and *O* correspond to those found in Ref. 40, and spectra *O*, *Q*, and *W* to those of Ref. 27. Very large, micron-sized clusters that show IR Mie scattering and the Christiansen effect have also been observed with our system and resemble spectra shown in Ref. 36. For generation of these clusters we

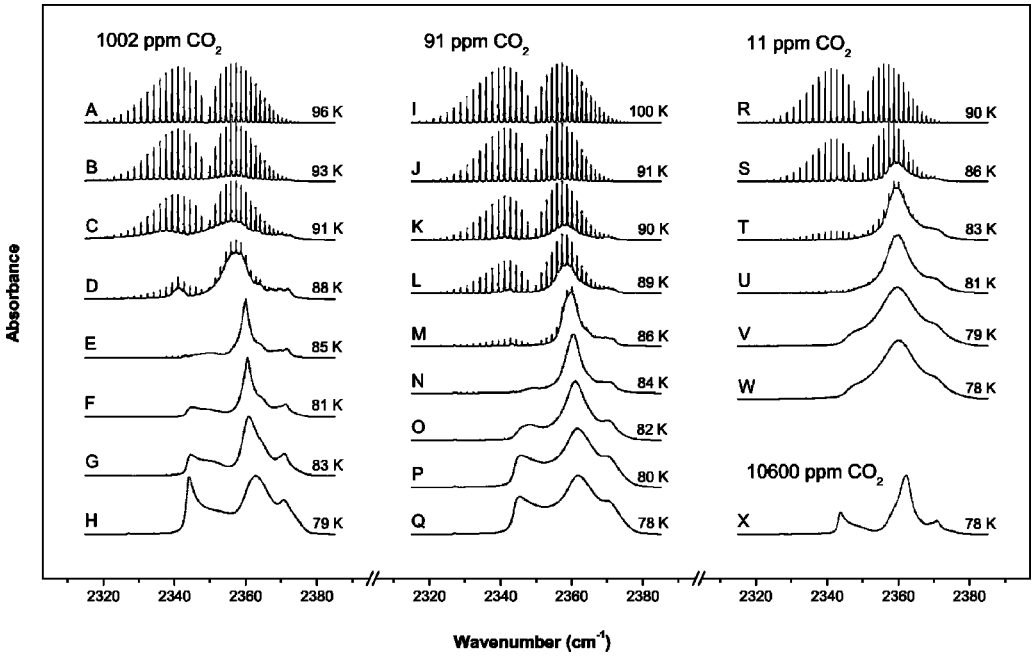

FIG. 5. FTIR spectra of CO_2 clusters. Three temperature sequences between 100 and 77 K were taken for the characterization of the vapor–solid phase transition. In each sequence gas pulses of 50 ms duration were injected into the cold buffer gas. Concentrations and pulse numbers were 1002 ppm, one pulse (left), 91 ppm, two pulses (center), and 11 ppm CO_2 in He, five pulses (right column). Buffer gas pressure was 200 mbar, optical path length 20 m, and spectral resolution 0.125 cm^{-1}. No buffer gas flow was used. For the spectrum at the lower right the concentration was 10 600 ppm, the other parameters remain unchanged. Cluster formation starts between 94 and 89 K. There are clear trends visible in the structure of the spectra. An exception is the sequence of spectra *F* and *G* for which, however, no assignment error or other error could be found. Spectral structure such as the formation of ''hooks'' in the outer parts of the spectra increase in complexity with increasing concentration. IR spectra of CO_2 found in the literature fit well into the series of spectra observed here. A simple estimate based on the SNR of the third series of measurements shows that clusters are probably still visible at concentrations 1000 times smaller than the one used here. Those clusters will then contain relatively few monomer molecules.

used concentrations in the percent range and injection pulse lengths of seconds or continuous sample gas injection.

The crystallographic structure of the many types of CO_2 aggregates produced in supersonic jets was identified with electron diffraction techniques as face-centered cubic (fcc).[72,73] In a more recent article other structures were found as well, particularly for small structures of about 100 monomer molecules.[74] Barnes *et al.* believe that structures other than fcc structures are possible as well for large aggregates.[35] Another consequence of the analysis of Maxwell's equations for the interaction of light with spherical particles by these authors is that the great variation in spectral structure and shape is indicative of sharp edges and corners on the particles. Our two-dimensional temperature-concentration diagram of Fig. 5 shows clearly that the conspicuous spectral structures such as the ''hook'' at 2345 cm^{-1} in spectrum *H* or the peak-and-valley structure at 2370 cm^{-1} in spectrum *D* get less pronounced as the concentration of the sample gas decreases. In the third series with 11 ppm CO_2 in He the hooks at 2345 and 2370 cm^{-1} are only visible as faint shoulders.

Although previous authors only saw solid CO_2 clusters, molecular dynamic simulations predict a dynamic coexistence of ''solidlike'' and ''liquidlike forms''[75] for $n=12$ to 14, and an aggregate with ordered core and liquid outer layers for $n=146$.[76] The clusters seen in the spectra of Fig. 5 contain considerably more than 100 monomer molecules each. Liquid or liquidlike components in individual clusters, if present at all, should be most likely close to the transition point from the gas to the solid phase, i.e., in spectra *B,C,D, K,L,M,S* or *T*. In spectrum *C* there is indeed a distinct peak near 2337 cm^{-1} that shifts to 2340 cm^{-1} and gets somewhat narrower in *D*. This structure is less pronounced in the two other series in *K,L,M* and in *S* and *T*, with decreasing tendency. Relative to the fundamental ν_3 vibration of the CO_2 monomer at 2349 cm^{-1} this structure is redshifted by 9–12 wave numbers. The cluster main structure at 2360 cm^{-1}, on the other hand, shifts by 11 cm^{-1} to the blue. It appears unlikely to us in view of the discussion on CO that glassy structures can form at these relatively high temperatures.

The smallest clusters are those presented in spectra *V* and *W* of Fig. 5. These were taken at the smallest sample gas concentration of 11 ppm. The signal-to-noise ratio (SNR) here is 2000 and can be considerably enhanced if longer measurement times and optical filters are used and if spectral resolution is reduced to perhaps 0.25 cm^{-1}. We thus estimate that with the present cooling technique cluster spectra can be investigated even with sample gas concentrations 1000 times lower than the ones used, i.e., with 10 ppb CO_2 in helium. We therefore expect to be able to produce and study by IR spectroscopy clusters that are much smaller in size than the ones previously investigated.

VI. DISCUSSION AND OUTLOOK

In molecular-cluster physics we have so far been in a situation where the advanced state to which simulation and theory had developed was not nearly matched by experimen-

tal work.[13] The cooling method described in this article provides experimental possibilities to close this gap. Conventional collisional cooling systems usually work with liquid nitrogen and thus allow a reduction of temperature by no more than a factor of 4, whereas a factor of 70 is reached with the present arrangement. Although there have been other liquid-helium cooled cells described in the literature,[51,52] the present system, with its 20 m of optical path length for FTIR applications, offers an optical absorption length 2–3 orders of magnitude higher, with a corresponding increase in sensitivity. The advantage of the present system over those using supersonic beam expansion with slit nozzles[1,18] or multireflection optics[77] is similar. Combined with the pulsed gas inlet system which allows rapid cooling of the sample gas, the temperature range between 4 and 80 K offers many possibilities for the investigation of new cluster systems having a wide variety of thermodynamic properties including a glassy structure.

That the results obtained with the new method can be important is perhaps best depicted with the structural change we observed in CO cluster spectra at temperatures between 20 and 5 K (cf. Fig. 4). To our knowledge this is the first time that collision-cooled molecular clusters in thermal equilibrium have been investigated with IR-spectrometric methods in that temperature region. The results suggest that, in addition to CO, other molecules should be amenable as well to a study of cluster formation including changes in structural order. In fact, the cooling to temperatures where cluster formation occurs will be much more rapid, under otherwise unchanged experimental conditions, for other substances with higher temperatures of evaporation, thus increasing the probability of formation of glassy aggregates.

Because of the long optical paths available the present system offers higher sensitivity than previous ones, allowing sub-ppm sample gas concentrations to be used, which is advantageous for the investigation of small clusters. The SNR of spectra *V* and *W* of Fig. 5 allows sample gas concentrations down to 10 ppm to be used for the observation of cluster formation. From kinetic gas theory,[78] it can easily be concluded that for the ppb sample gas concentrations used in our system the average time between collisions at 5 K is on the order of several seconds. At these temperatures monomers should thus be amenable to sensitive detection by both FTIR and TDL spectroscopy.[50,51] The same is true for very small clusters to an even higher degree.

The precise control of the experiment temperature is particularly important when changes in structural order of clusters are to be observed. This can directly be seen from Fig. 5. Small temperature changes on the order of 1 K lead to considerable changes in the spectral structures, especially at high sample gas concentrations. Our experiments show that temperature, sample gas concentration, and cooling speed are the most critical parameters for cluster formation in collisional cooling. A meaningful presentation of the results is therefore a four-dimensional graphical arrangement of spectra (absorbance A versus wave number ν) grouped by temperature T and sample gas number density N. A fifth quantity of interest is time t, which directly describes the cluster formation process and can indirectly be used to get hold on the cooling velocity and its effects on the resulting cluster structures.[79]

The three zones of the present cooling cell allow us to submit the clusters to a temperature program. They can be heated and cooled at will during their lifetime or made to flow through zones with a temperature gradient. This includes the possibility of applying processes such as annealing, surface melting, and recrystallization. Such processes have been dealt with in simulations, but few experimental investigations have so far been reported.[71]

The possibility of adjusting and controlling the temperature of the mirrors not only allows us to avoid, but also to purposely induce the deposit of sample gas on the mirrors and to have the deposit melt, recrystallize, and evaporate. This can provide additional information on properties of the bulk material. In addition to being operated with continuous and pulsed gas inlet, the cell can also be used as a sensitive diffusion cloud chamber[80] by maintaining the bottom of the cell at a higher temperature than the top, thus forcing the contents to circulate and undergo circulation-induced nucleation.

Our activities in the near future will be directed toward the combination of the possibilities of generating clusters of a different kind with a more direct determination of their size using effects such as light scattering, sedimentation,[28] and distinct reactions of monomer molecules on the cluster surfaces, either of the same[81] or of a different kind[42] than that of which the bulk of the cluster is made up. Another interesting field is probably the investigation of the effect of ultrasound, not just on large clusters that form from smaller clusters in a second-order process[82,83] but on directly generated primary clusters from the gas phase as well. We finally believe that the described method could provide complementary information on the rapidly developing field of molecular and cluster spectroscopy in cold helium droplets.[84–86]

ACKNOWLEDGMENTS

Our thanks are due to B. Neidhart for his continued interest, encouragement, and support. We appreciate fruitful discussions with and practical suggestions by M. Kunzmann, W. Lahmann, R. Signorell, and R. Tuckermann. We thank M. Suhm for very constructive criticism. We gratefully acknowledge the help of W. Schieder and H. Böttcher who shared their technological experience with us and supported this work. This article is dedicated to Prof. Dr.-Ing. Bernd Neidhart on the occasion of his 60th birthday.

[1] M. Herman, R. Georges, M. Hepp, and D. Hurtmans, Int. Rev. Phys. Chem. **19**, 277 (2000).
[2] *Tunable Diode Laser Spectroscopy 1998*, edited by A. W. Mantz (Elsevier, Amsterdam, 1999).
[3] *Atmospheric and Planetary Spectroscopy*, edited by C. Chackerian (Pergamon, Oxford, 1992).
[4] J.-L. Le Garrec, B. R. Rowe, J. L. Queffelec, J. B. A. Mitchell, and D. C. Clary, J. Chem. Phys. **107**, 1021 (1997).
[5] M. Quack and J. Stohner, Phys. Rev. Lett. **84**, 3807 (2000).
[6] F. F. Abraham, *Homogeneous Nucleation Theory* (Academic, New York, 1974).
[7] U. Buck, J. Phys. Chem. **98**, 5190 (1994).
[8] *Clusters of Atoms and Molecules*, edited by H. Haberland (Springer, Berlin, 1994).
[9] Z. Bacic and R. E. Miller, J. Phys. Chem. **100**, 12945 (1996).
[10] P. K.Chakraborti, *Molecular and Cluster Physics*, edited by S. A. Ahmad (Narosa, New Delhi, 1997).

[11] E. W. Schlag, *Molecular Clusters* (Elsevier, Amsterdam, 1998).
[12] J. Jellinek, *Theory of Atomic and Molecular Clusters* (Springer, Berlin, 1999).
[13] R. S. Berry, *Theory of Atomic and Molecular Clusters*, edited by J. Jellinek (Springer, Berlin, 1999).
[14] N. K. Wilson and J. W. Childers, Appl. Spectrosc. Rev. **25**, 1 (1989).
[15] E. Knözinger and P. Beichert, J. Phys. Chem. **99**, 4906 (1995).
[16] P. B. Davies and A. J. Morton-Jones, Appl. Phys. B: Photophys. Laser Chem. **42**, 35 (1987).
[17] T. Häber, U. Schmitt, and M. A. Suhm, Phys. Chem. Chem. Phys. **1**, 5573 (1999).
[18] T. Häber, U. Schmitt, C. Emmeluth, and M. A. Suhm, Faraday Discuss. (2001).
[19] J. B. Anderson, R. P. Andres, and J. B. Fenn, Adv. Chem. Phys. **10**, 275 (1966).
[20] G. Herzberg, Astrophys. J. **115**, 337 (1952).
[21] A. Watanabe and H. L. Welsh, Can. J. Phys. **43**, 818 (1965).
[22] J. U. White, J. Opt. Soc. Am. **32**, 285 (1942).
[23] R. P. Blickensderfer, G. E. Ewing, and R. Leonard, Appl. Opt. **7**, 2214 (1968).
[24] A. R. W. McKellar, N. Rich, and V. Soots, Appl. Opt. **9**, 222 (1970).
[25] A. R. W. McKellar and H. L. Welsh, Can. J. Phys. **50**, 1458 (1972).
[26] A. R. W. McKellar, J. Chem. Phys. **92**, 3261 (1990).
[27] G. E. Ewing and D. T. Sheng, J. Phys. Chem. **92**, 4063 (1988).
[28] R. Disselkamp and G. E. Ewing, J. Chem. Phys. **99**, 2439 (1993).
[29] K. C. Kim, E. Griggs, and W. B. Person, Appl. Opt. **17**, 2511 (1978).
[30] K. C. Kim and M. J. Reisfeld, Appl. Spectrosc. **39**, 1056 (1985).
[31] J. Ballard, K. Strong, J. J. Remedios, M. Page, and W. B. Johnston, J. Quant. Spectrosc. Radiat. Transf. **52**, 677 (1994).
[32] A. S. Pine and W. J. Lafferty, J. Chem. Phys. **78**, 2154 (1983).
[33] K. von Puttkamer and M. Quack, Chem. Phys. **139**, 31 (1989).
[34] J. A. Barnes, T. E. Gough, and M. Stoer, Rev. Sci. Instrum. **60**, 406 (1989).
[35] J. A. Barnes, T. E. Gough, and M. Stoer, J. Chem. Phys. **95**, 4840 (1991).
[36] J. A. Barnes, T. E. Gough, and M. Stoer, J. Phys. Chem. **97**, 5495 (1993).
[37] T. E. Gough and T. Wang, Chem. Phys. Lett. **207**, 517 (1993).
[38] T. E. Gough and T. Wang, J. Chem. Phys. **102**, 3932 (1995).
[39] P. Varanasi and S. Chudamani, J. Mol. Spectrosc. **134**, 440 (1989).
[40] F. Fleyfel and J. P. Devlin, J. Phys. Chem. **93**, 7292 (1989).
[41] B. Rowland, M. Fisher, and J. P. Devlin, J. Phys. Chem. **97**, 2485 (1993).
[42] J. Sadlej, B. Rowland, J. P. Devlin, and V. Buch, J. Chem. Phys. **102**, 4804 (1995).
[43] T. Dunder and R. E. Miller, J. Chem. Phys. **93**, 3693 (1990).
[44] T. Dunder, M. L. Clapp, and R. E. Miller, J. Geophys. Res. **98**, 1213 (1993).
[45] D. Newnham, J. Ballard, and M. Page, Rev. Sci. Instrum. **66**, 4475 (1995).
[46] K. M. Smith, G. Duxburry, D. A. Newnham, and J. Ballard, J. Chem. Soc., Faraday Trans. **93**, 2735 (1997).
[47] M. Loewenstein and H. W. Wilson, Spectrochim. Acta, Part A **48**, 1243 (1992).
[48] M. A. H. Smith and C. P. Rinsland, Spectrochim. Acta, Part A **48**, 1257 (1992).
[49] D. Romanini and K. K. Lehmann, J. Mol. Spectrosc. **151**, 54 (1992).
[50] D. R. Willey, K. A. Ross, V. Dunjko, and A. W. Mantz, J. Mol. Spectrosc. **168**, 301 (1994).
[51] D. R. Willey, K. A. Ross, A. S. Mullin, S. Schowen, L. Zheng, and G. Flynn, J. Mol. Spectrosc. **169**, 66 (1995).
[52] Y. Abebe, C. D. Ball, F. C. De Lucia, and A. W. Mantz, Spectrochim. Acta, Part A **55**, 1957 (1999).
[53] D. R. Willey, R. L. Crownover, D. N. Bittner, and F. C. De Lucia, J. Chem. Phys. **89**, 1923 (1988).
[54] E. R. Kerstel and G. Scoles, Anal. Phys. Inorg. Chem. **2**, 178 (1990).
[55] D. R. Willey, R. E. Timlin, Jr., M. Deramo, P. L. Pondillo, D. M. Wesolek, and R. W. Wig, J. Chem. Phys. **113**, 611 (2000).
[56] M. Mengel, D. C. Flatin, and F. C. De Lucia, J. Chem. Phys. **112**, 4069 (2000).
[57] C. D. Ball and F. C. De Lucia, Phys. Rev. Lett. **81**, 305 (1998).
[58] J. K. Messer and F. C. De Lucia, Phys. Rev. Lett. **53**, 2555 (1984).
[59] S. Bauerecker, F. Taucher, C. Weitkamp, W. Michaelis, and H. K. Cammenga, in *Monitoring of Gaseous Pollutants by Tunable Diode Lasers*, edited by R. Grisar, H. Böttner, M. Tacke, and G. Restelli (Kluwer Academic, Dordrecht, 1992), p. 291.
[60] S. Bauerecker and H. K. Cammenga, Internationale Patent No. PCT/DE92/00843, (5 October 1992); Patent No. DE4133701A1 (15 April 1993).
[61] S. Bauerecker, PhD dissertation, TU Braunschweig, Geesthacht, 1995.
[62] S. Bauerecker, F. Taucher, C. Weitkamp, W. Michaelis, and H. K. Cammenga, J. Mol. Struct. **348**, 237 (1995).
[63] F. Taucher, C. Weitkamp, W. Michaelis, H. K. Cammenga, and S. Bauerecker, J. Mol. Struct. **348**, 243 (1995).
[64] S. Bauerecker *et al.* (unpublished).
[65] *CRC Handbook of Chemistry and Physics*, 64th ed., edited by R. C. Weast, M. J. Astle, and W. H. Beyer (Chemical Rubber Corp., Boca Raton, FL, 1983).
[66] A. Givan, A. Loewenschuss, and C. J. Nielsen, Vib. Spectrosc. **16**, 85 (1998).
[67] M. Havenith, M. Petri, C. Lubina, G. Hilpert, and W. Urban, J. Mol. Spectrosc. **167**, 248 (1994).
[68] L. S. Bartell and J. Chen, J. Phys. Chem. **96**, 8801 (1992).
[69] D. Baumer and E. Riedel, *Gase Handbuch* (Messer Griesheim, Frankfurt, 1989).
[70] J. P. Devlin, C. Joyce, and V. Buch, J. Phys. Chem. **104**, 1974 (2000).
[71] M. L. Clapp, R. E. Miller, and D. R. Worsnop, J. Phys. Chem. **99**, 6317 (1995).
[72] G. Torchet, H. Bouchier, J. Farges, M.-F. de Feraudy, and B. Raoult, J. Chem. Phys. **81**, 2137 (1984).
[73] L. S. Bartell, Chem. Rev. **86**, 491 (1986).
[74] G. Torchet, M.-F. de Feraudy, A. Boutin, and A. H. Fuchs, J. Chem. Phys. **105**, 3671 (1996).
[75] J.-B. Maillet, A. Boutin, and A. H. Fuchs, Mol. Simul. **19**, 285 (1997).
[76] G. Cardini, V. Schettino, and M. L. Klein, J. Chem. Phys. **90**, 4441 (1989).
[77] D. McNaughton, D. McGilvery, and E. G. Robertson, J. Chem. Soc., Faraday Trans. **90**, 1055 (1994).
[78] F. Reif, *Fundamentals of Statistical and Thermal Physics* (De Gruyter, Berlin, 1985).
[79] M. K. Kunzmann, R. Signorell, M. Taraschewski, and S. Bauerecker, Phys. Chem. Chem. Phys. **3**, 3742 (2001).
[80] P. P. Wegener, Naturwissenschaften **74**, 111 (1987).
[81] B. Rowland and J. P. Devlin, J. Chem. Phys. **94**, 812 (1991).
[82] S. Bauerecker and B. Neidhart, J. Chem. Phys. **109**, 3709 (1998).
[83] S. Bauerecker and B. Neidhart, Science **282**, 2211 (1998).
[84] M. Hartmann, R. E. Miller, J. P. Toennies, and A. F. Vilesov, Science **268**, 1631 (1996).
[85] M. Behrens, R. Froechtenicht, M. Hartmann, J.-G. Siebers, U. Buck, and F. C. Hagemeister, J. Chem. Phys. **111**, 2436 (1999).
[86] K. Nauta and R. E. Miller, Science **287**, 293 (2000).